Science Signaling
AAAS

www.sciencesignaling.org/cgi/content/full/5/254/ra90/DC1

Supplementary Materials for

TIM Family Proteins Promote the Lysosomal Degradation of the Nuclear Receptor NUR77

Savithri Balasubramanian,* Satya Keerthi Kota, Vijay K. Kuchroo, Benjamin D. Humphreys, Terry B. Strom*

*To whom correspondence should be addressed. E-mail: skota@bidmc.harvard.edu (S.B.); tstrom@bidmc.harvard.edu (T.B.S.)

Published 11 December 2012, *Sci. Signal.* **5**, ra90 (2012)
DOI: 10.1126/scisignal.2003200

The PDF file includes:

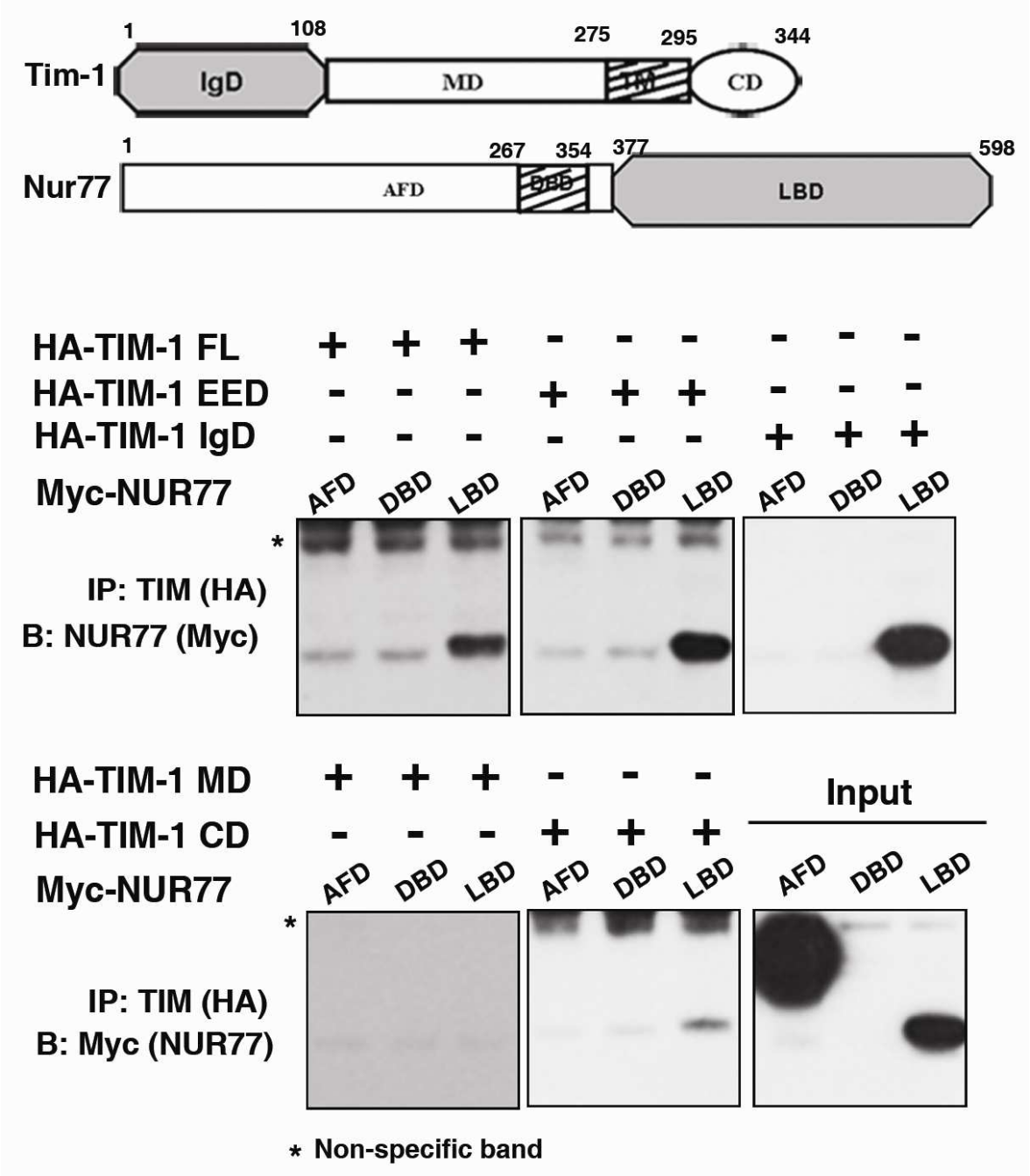

Figure S1. NUR77 domains required for the interaction with TIM-1. The ligand binding domain of NUR77 mediates its interaction with TIM-1, demonstrated by coimmunoprecipitation assay of pair-wise combinations of various domains of HA-tagged TIM-1 (FL: full length; EED: entire extracellular domain comprising of IgV and mucin domains; IgVD: IgV domain; MD: mucin domain; CD: cytoplasmic domain) and myc-tagged domains of NUR77 (AFD: activation function domain; DBD: DNA binding domain; LBD: ligand binding domain). N=2 independent experiments.

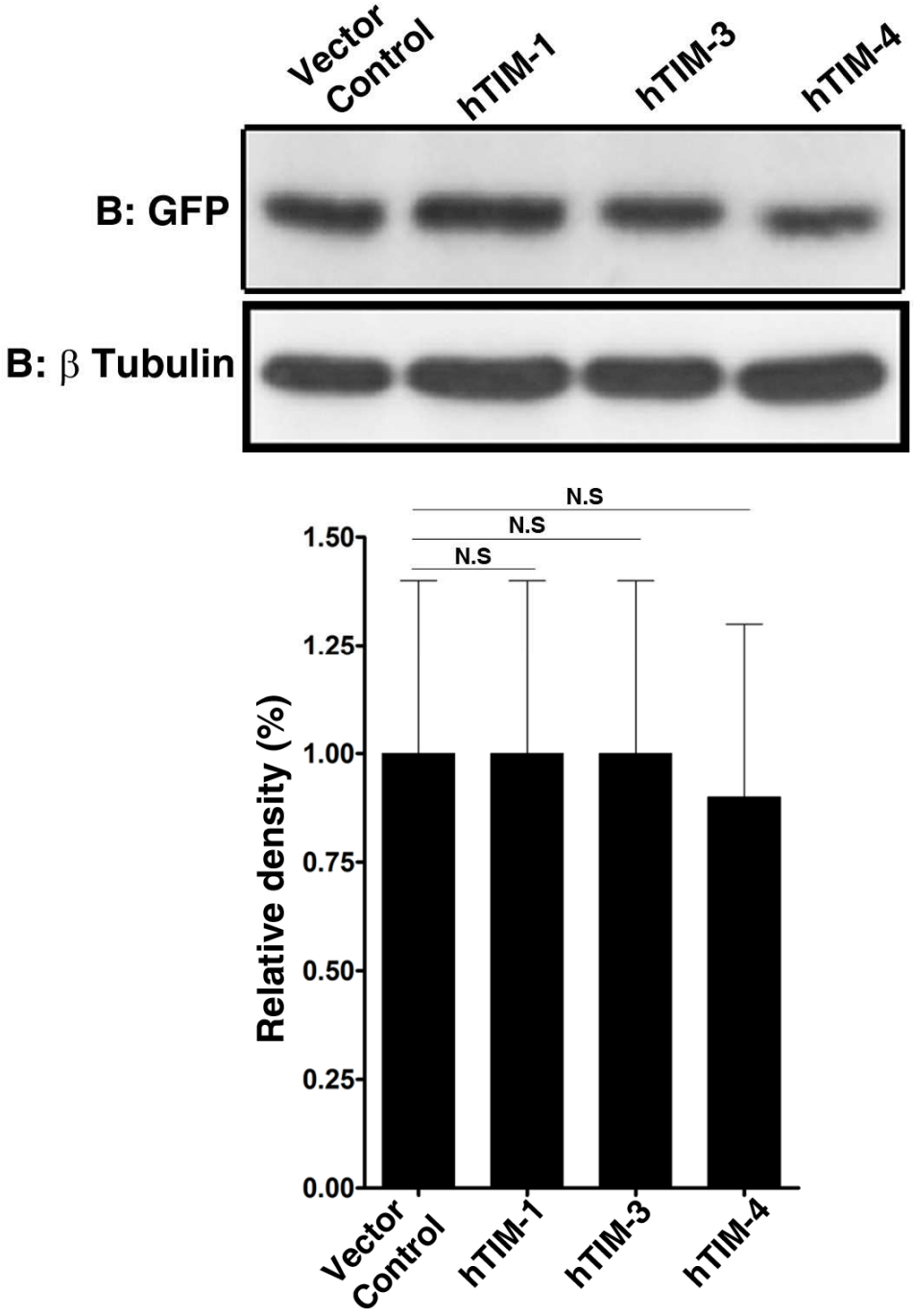

Figure S2. TIM proteins do not affect the abundance of GFP. Top panel: Representative western blot depicting the lack of change in GFP abundance in the presence and absence of TIM proteins. Bottom panel: Quantitation of protein density of GFP from three independent experiments.

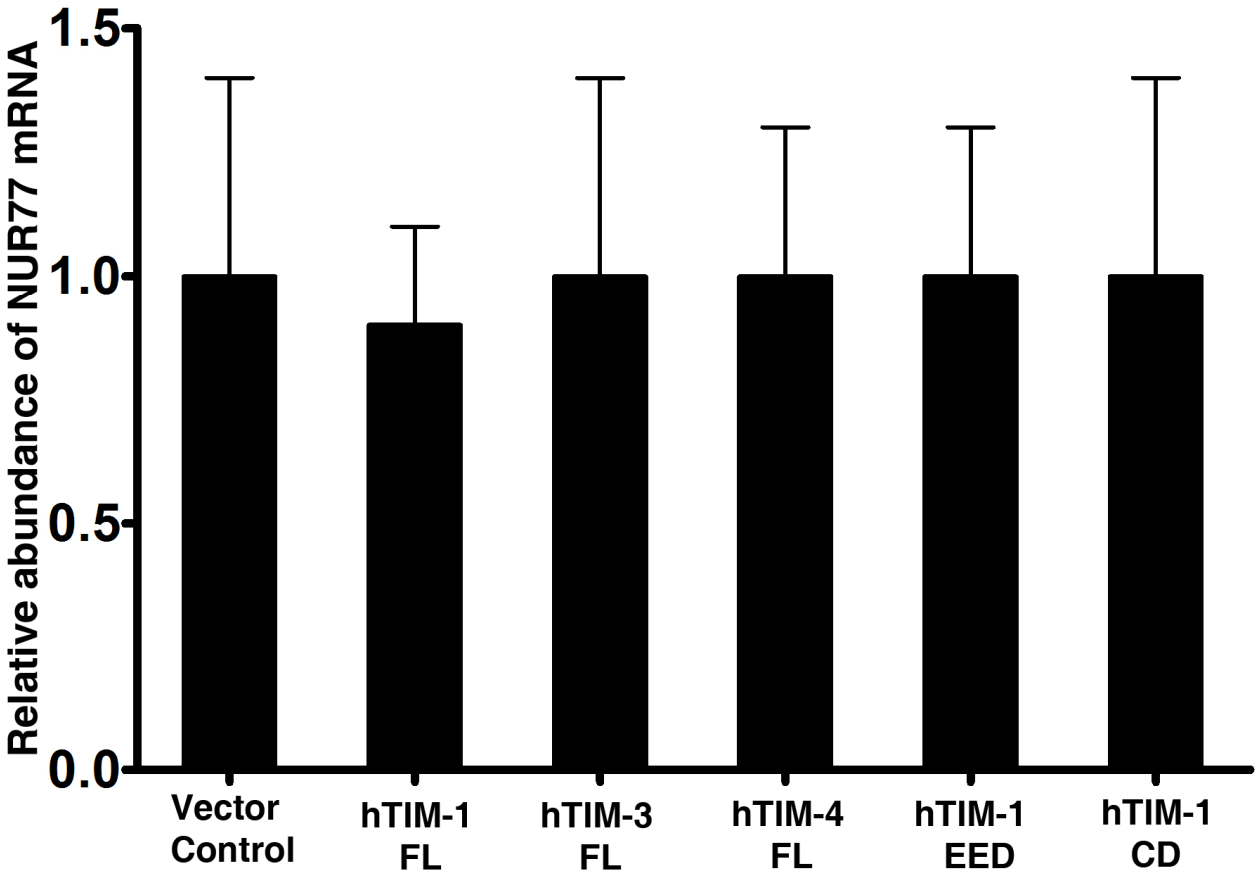

Figure S3. Reduction of NUR77 protein abundance is not through squelching. TIM protein-mediated reduction in NUR77 protein abundance is not a result of squelching, as demonstrated by the qRT-PCR measurement of RNA abundance of NUR77 in the presence of full length TIM-1, -3, -4 and deletion constructs of TIM-1. N=3 independent experiments.

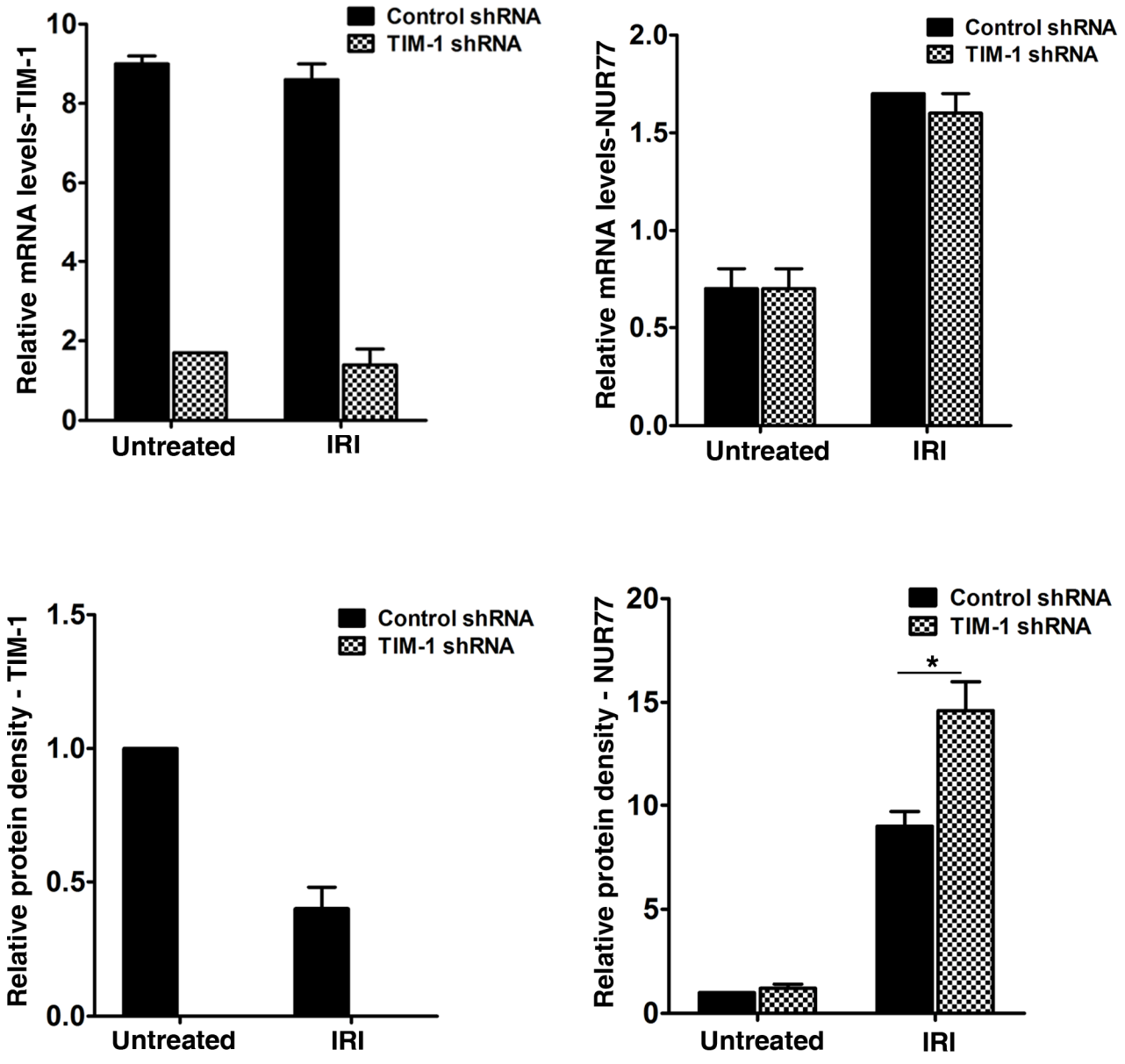

Figure S4. Silencing of TIM-1 increases NUR77 protein abundance in HK-2 cells in an in vitro epithelial cell injury model. Human renal tubular epithelial cells, HK2 that were stably transfected with either control shRNA or TIM-1 shRNA were subjected to injury using a cocktail of antimycin A, 2-deoxyglucose and A23187 that results in cellular apoptosis. TIM-1 RNA and protein are present under steady state conditions in HK-2 cells, whereas NUR77 is induced both at the RNA and protein levels upon injury. Silencing of TIM-1 significantly increased the abundance of NUR77 protein (bottom panel) whereas NUR77 transcripts were induced to the same extent (top panel). N=3 independent experiments.

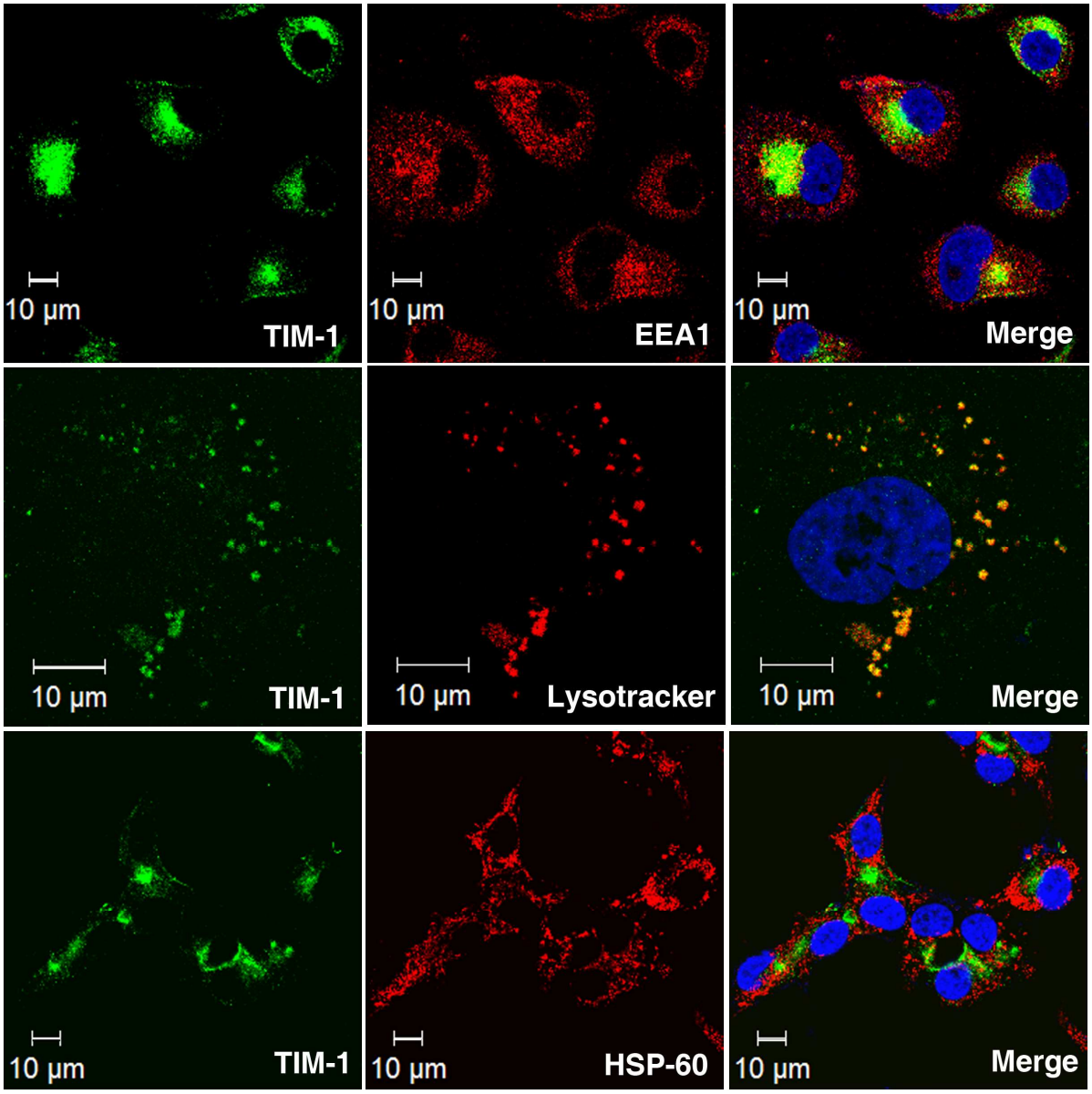

Figure S5. Cellular localization of endogenous TIM-1. Colocalization of endogenously expressed TIM-1 in 769-P cells with markers of early endosomes (EEA1) and lysosomes (Lysotracker) and not with a marker for mitochondria (HSP60). Scale bar: 10 µm. Colocalization coefficients: hTIM-1/EEA1: 0.49±0.06; hTIM-1/Lysotracker: 0.75±0.04; hTIM-1/HSP-60: 0.08±0.01; n=5 cells each from two independent experiments.

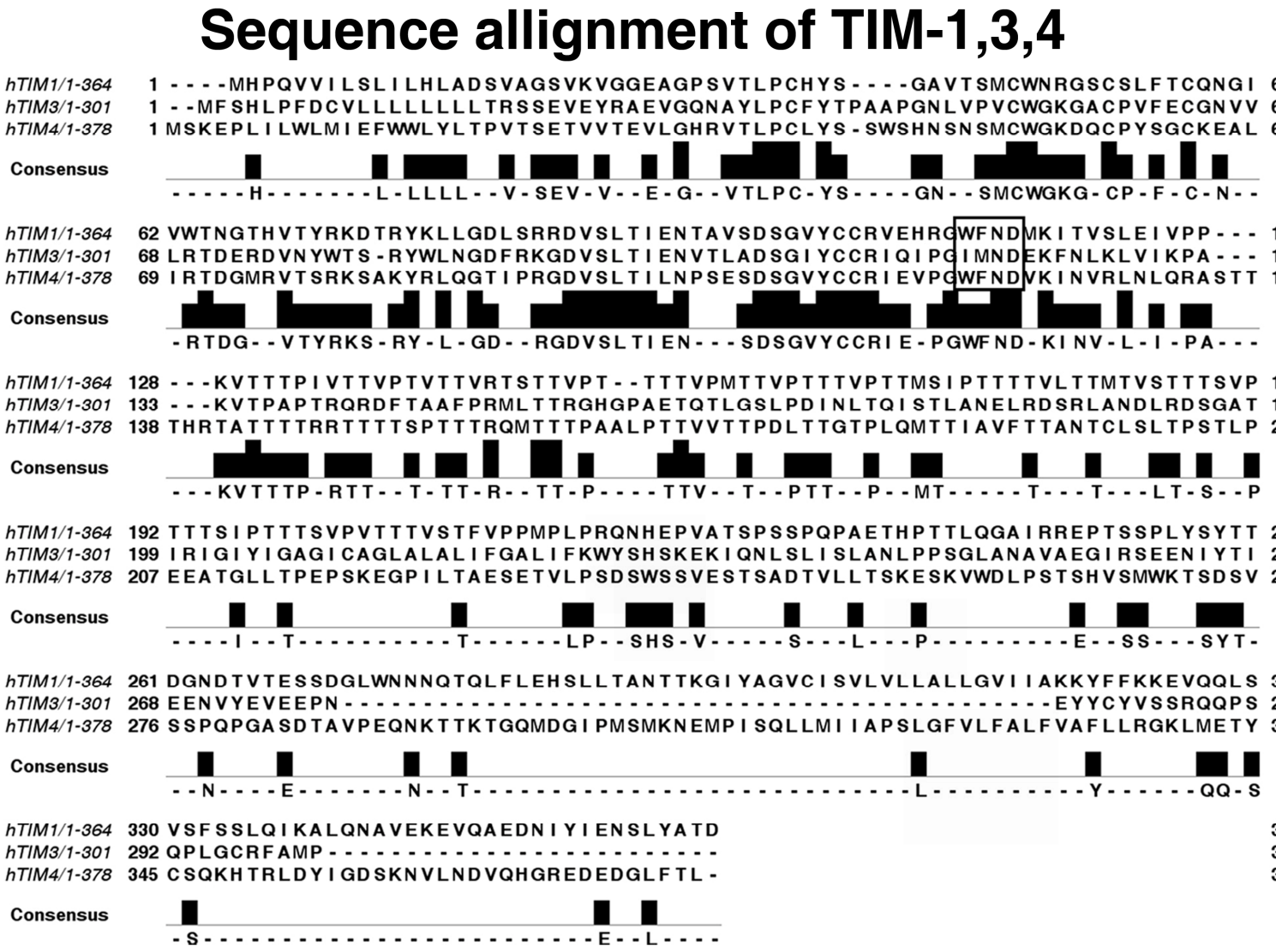

Figure S6. The IgV domain of TIM proteins is highly conserved. Sequence alignment of human TIM family proteins (TIM-1, -3 and -4), revealing high identity at the amino acid level in the IgV domain. Residues in the MILIBS are boxed.

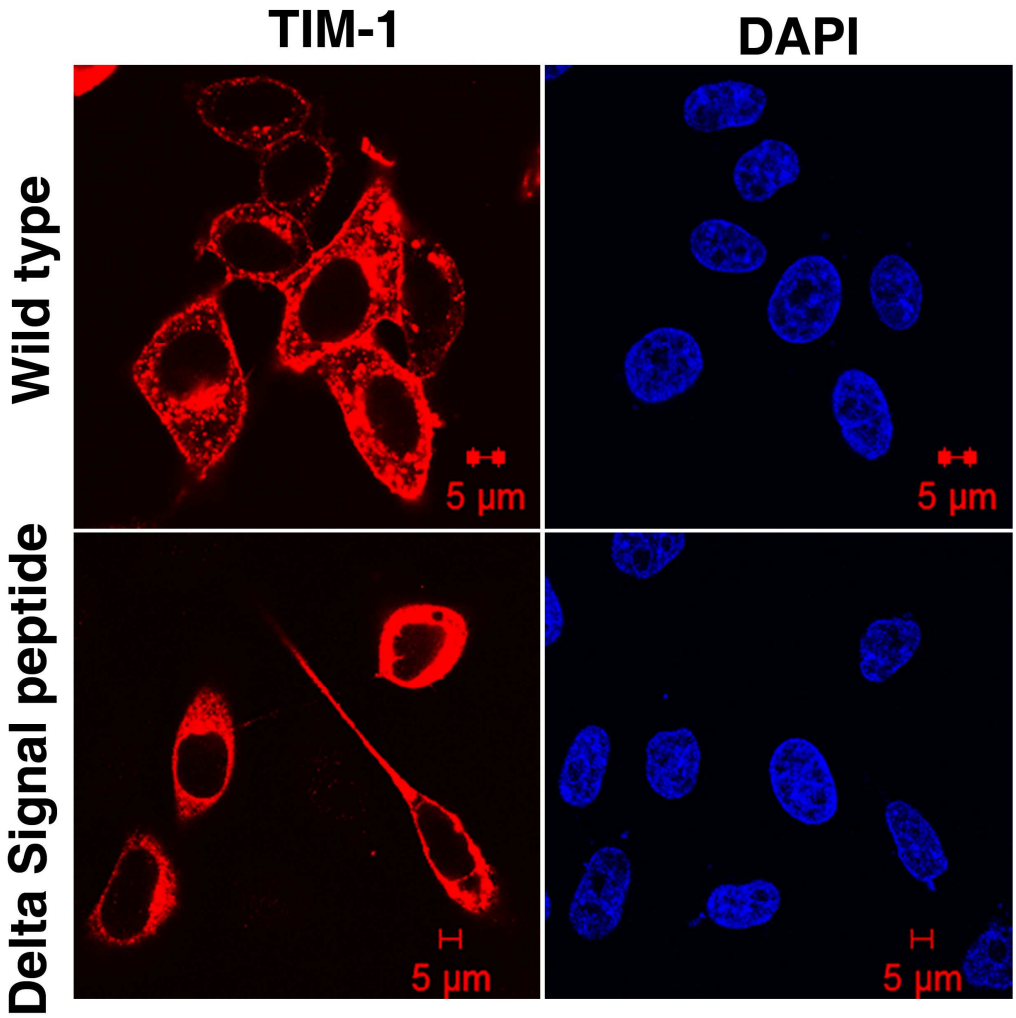

Figure S7. Localization pattern of wild-type and signal peptide–deleted TIM-1 proteins. Wild-type TIM-1 presented a cell surface as well as vesicular staining pattern, whereas the signal peptide-deleted TIM-1 was apparently not targeted to plasma membrane and distributed homogenously in the cytoplasm. Scale bar: 10 µm. N=2 independent experiments.

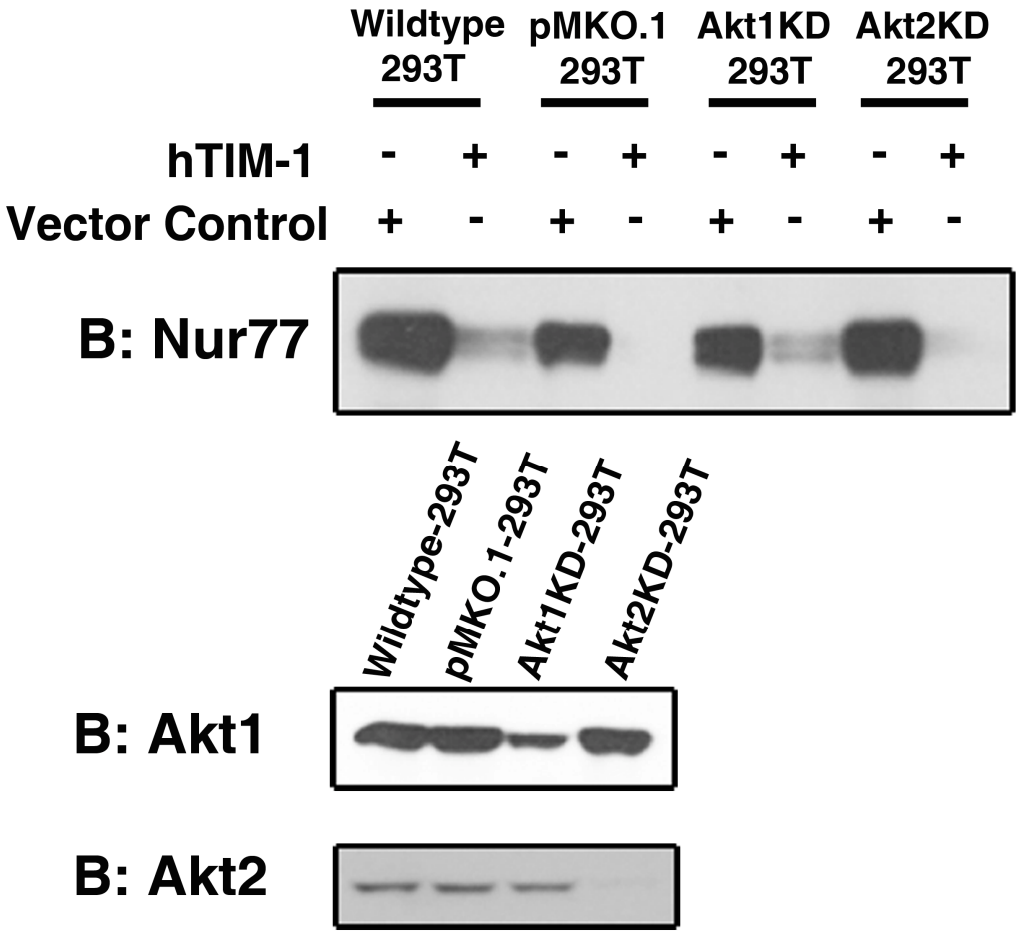

Figure S8. The requirement for PI3K in TIM-1–mediated degradation of NUR77 is independent of Akt signaling. Wild-type, vector control (pMKO.1), Akt1 knockdown (Akt1KD) or Akt2 knockdown (Akt2KD) stable lines of 293T cells were co-transfected either vector control or full length TIM-1 along with GFP-NUR77 and the abundance of NUR77 was analyzed by Western blot analysis. Presence or absence of Akt isoforms did not appear to alter the magnitude of TIM-1 mediated NUR77 degradation (top panel). Bottom panel depicts the abundance of Akt1 and Akt2 in the stable knockdown lines. N=2 independent experiments.

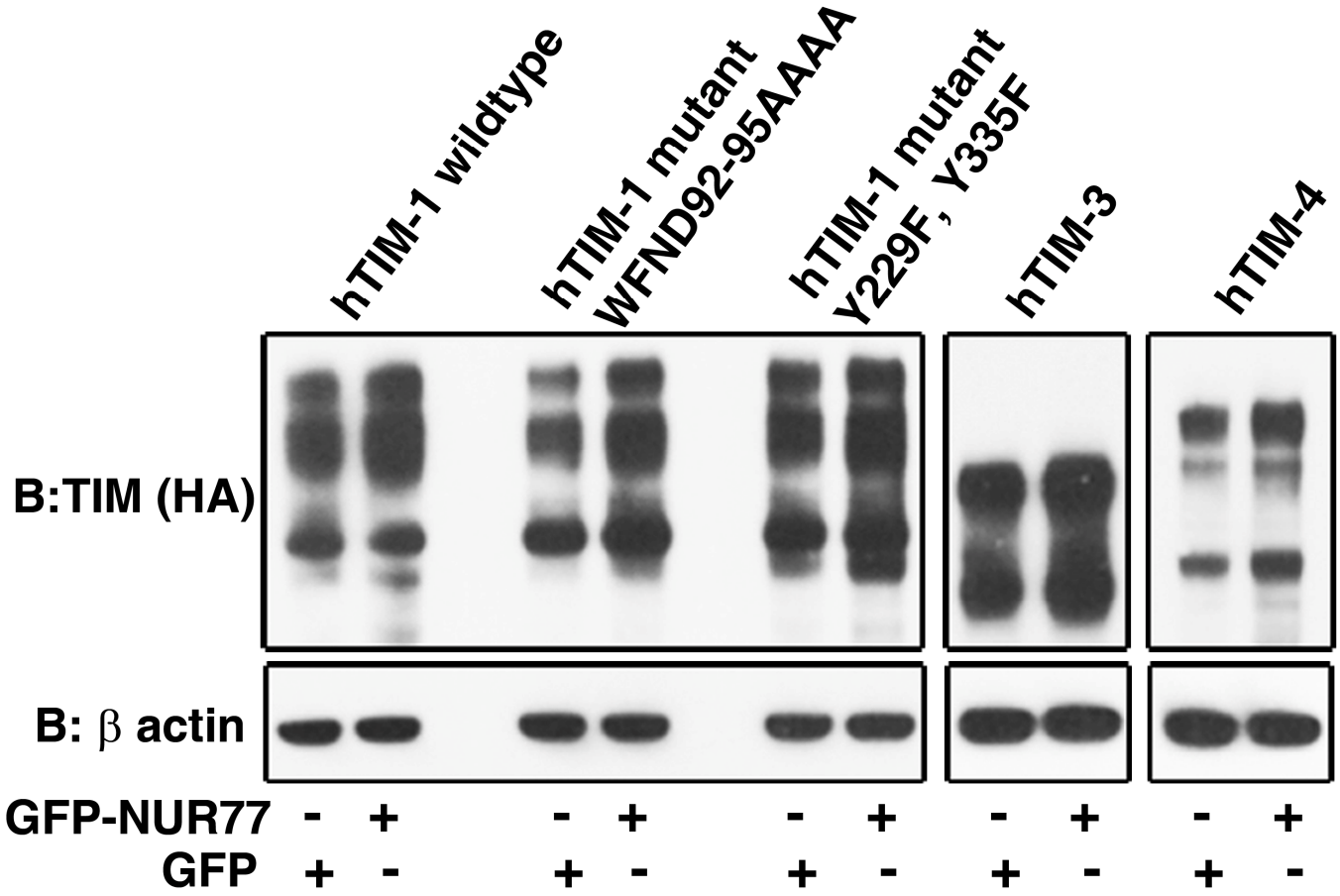

Figure S9. TIM-1 is not subjected to lysosomal degradation. Protein abundance of wild-type, the MILIBS mutant (WFND92-95AAAA) and cytoplasmic double tyrosine mutant (Y299F, Y335F) of TIM-1, and full length TIM-3 and TIM-4 are not altered during the process of degradation of NUR77 degradation. N=2 independent experiments.

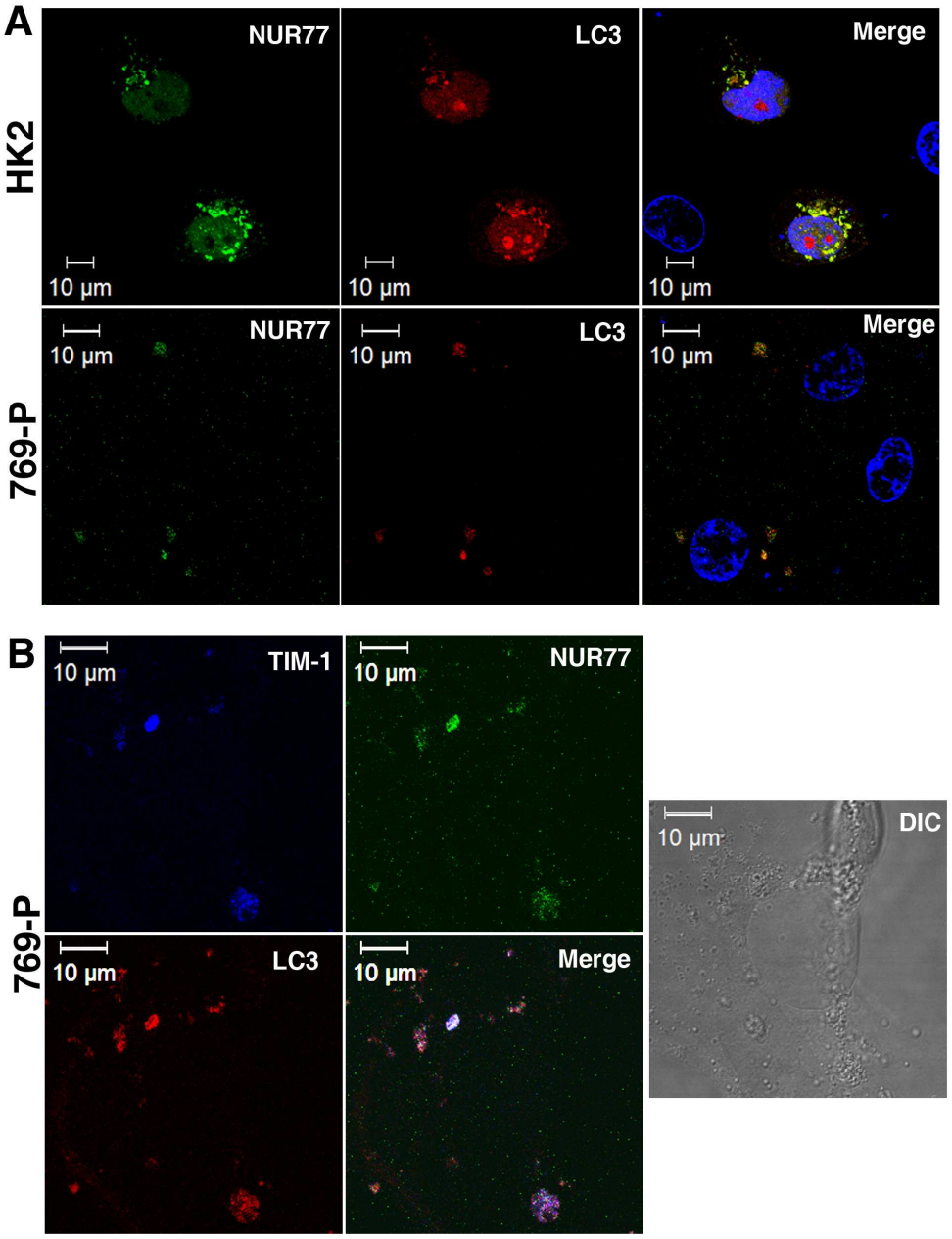

Figure S10. Colocalization of NUR77 and TIM-1 with the autophagosome marker LC3. (A and B) Colocalization of NUR77 with the autophagosomes marker LC3 in HK2 and 769-P cells (A). Colocalization coefficients- NUR77/LC3: 0.71±0.05 (HK-2); 0.62±0.04 (769-P). 769-P cells were transiently transfected with GFP-NUR77 and RFP-LC3 and stained for endogenous TIM-1 (B). Colocalization coefficients: hTIM-1/LC3: 0.78±0.02; NUR77/LC3: 0.74±0.03; hTIM-1/NUR77: 0.76±0.04; n=5 cells each from two independent experiments. Scale bar: 10 µM.

Table S1. Interacting partners of hTIM-1 identified in the yeast two-hybrid screen.

Interacting partners for human TIM-1 IgV domain	**Accession number**
Homo sapiens nuclear receptor subfamily 4, group A, member 1 (NR4A1), transcript variant 1	NM_002135.3
Homo sapiens nuclear receptor interacting protein 2 (NRIP2)	NM_031474.1
Homo sapiens filamin A, alpha (actin binding protein 280) (FLNA)	NM_001456.1
Homo sapiens crystallin, alpha B (CRYAB), mRNA	NM_001885.1
Homo sapiens DnaJ (Hsp40) homolog, subfamily A, member 3 (DNAJA3)	NM_005147.3
Homo sapiens HLA-B associated transcript 3 (BAT3), transcript variant 2	NM_080702.1
Homo sapiens amplified in osteosarcoma (OS9), transcript variant 1	NM_006812.2
Homo sapiens chromosome 16 open reading frame 58 (C16orf58)	NM_022744.1